

Variable tomographic scanning with wavelength scanning digital interference holography

Lingfeng Yu *, Myung K. Kim

Department of Physics, PHY 114, University of South Florida, 4202 E. Fowler Avenue, Tampa, FL 33620, United States

Received 12 September 2005; received in revised form 25 October 2005; accepted 8 November 2005

Abstract

We present a new method for variable tomographic scanning based on the wavelength scanning digital interference holography (WSDIH). A series of holograms are generated with a range of scanned wavelengths. The object field is reconstructed in a number of selected tilted planes from each hologram, and the numerical superposition of all the tilted object fields results in a variable tomographic scanning. The scanning direction can be arbitrary angles in 3D space but not limited in a 2D plane, thus the proposed algorithm offers more flexibility for acquiring and observing randomly orientated features of a specimen in a WSDIH system. Experiments are performed to demonstrate the effectiveness of the method.

© 2005 Elsevier B.V. All rights reserved.

Keywords: Digital holography; Tomography; Three-dimensional image acquisition; Microscopy

1. Introduction

In contrast to conventional microscopy where the image of in-focus plane is superposed with blurred image of out-of-focus planes, three-dimensional microscopy that reveals the tomographic structure of the sample has found many applications in biological and materials science. Optical coherence tomography [1] (OCT) is a scanning microscopic technique that is suitable for high-resolution cross-sectional imaging. The basis of OCT is to detect the light scattered from an object that is illuminated by a light source of low temporal but high spatial coherence, and the three-dimensional image is reconstructed by scanning the sample area or volume pixel by pixel. Its axial resolution is determined by the source coherence length and its lateral resolution is determined by the numerical aperture of the sampling lens. Full-field two-dimensional OCT [2–6] has

also been reported as a technique to acquire two-dimensional tomographic images while maintaining the optical sectioning characteristics of OCT. With the illumination of a broadband light source, the regions of the image that do contain interferometric information can be extracted by digital processing of the CCD images, thus generating two-dimensional optical section images. Wavelength scanning digital interference holography (WSDIH) [7,8] is another 3D microscopy and tomographic imaging technique that we have been developing. By recording a series of holograms using a range of scanned wavelengths, and superposing image volumes from each of the holograms together, a synthesized short coherence length and corresponding axial resolution can be obtained.

The tomographic images reported in the above 3D microscopy systems however are all obtained with a fixed scanning direction parallel to the optical axis of the system. If the interesting feature is located on a plane not parallel to the scanning plane, it needs to be reconstructed by combining or interpolating points from different tomographic layers. However, if the lateral resolution does not match well with the axial resolution, the quality of the interpolated

* Corresponding author. Tel.: +1 813 974 1635; fax: +1 813 974 5813.
E-mail addresses: yulingfeng@gmail.com (L. Yu), mkkim@cas.usf.edu (M.K. Kim).

image will be greatly degraded. As in the above WSDIH system [7,8], the axial resolution is determined by the wavelength scanning range of the dye laser system and normally is on the order of $\sim 10 \mu\text{m}$. However, the lateral resolution can be much higher if microscopic objectives with high magnification are used in the optical system.

One approach to solve this problem is to physically repeat the whole process either with the reference mirror tilted or the object rotated to a desired orientation. However, this is time-consuming and cumbersome. We have proposed another novel approach called variable tomographic scanning [9] based on WSDIH. Since the advantage of digital holography is that a single hologram records the entire three-dimensional information of the object, it is possible to calculate more rigorous wavefield distributions directly on the tilted planes from the recorded holograms, thus the synthesized tilted tomographic images will have better quality than those only from interpolation. By this way, flexible selection and accurate reconstruction of scanning planes are possible, and the whole process can be fulfilled without physically tilting the object and recording the holograms again. However, only scanning directions within a 2D plane was reported, and the selection of the reconstruction planes limited in space, thus it will pose a restriction to the application of variable tomographic scanning. In this paper, we overcome the above-mentioned limitations and propose an algorithm to reconstruct wavefields on planes that are arbitrarily tilted in 3D space. Thus it offers more flexibility for acquiring and observing images of randomly orientated features of a specimen in a WSDIH system. Below in Section 2, we briefly review the principle of WSDIH and describe the detailed principles of variable tomographic scanning in 3D space. Some experimental results are presented in Section 3 to verify the proposed idea, and a conclusion is given in Section 4.

2. Principle

2.1. Wavelength scanning digital interference holography

The principle of wavelength scanning digital interference holography has been reported in [7,8]. Here we give a brief review of the principle. If a laser beam of wavelength λ is used to illuminate a volume object. Any point P on the object at \mathbf{r}_P scatters the incident beam into a Huygens wavelet $A(\mathbf{r}_P)$, so that the resultant field $E(\mathbf{r})$ at \mathbf{r} is

$$E(\mathbf{r}) \sim \int A(\mathbf{r}_P) \exp(ik|\mathbf{r} - \mathbf{r}_P|) d^3\mathbf{r}_P, \quad (1)$$

where the integral is over the whole object volume. A digital camera is used to record a hologram. It contains both the amplitude and phase information of the object, and can be used to reconstruct its wave propagation at different positions. If the holographic process is repeated using N different wavelengths, and the reconstructed fields are all superposed together, then the resultant field is

$$\begin{aligned} E(\mathbf{r}) &\sim \sum_k \int A(\mathbf{r}_P) \exp(ik|\mathbf{r} - \mathbf{r}_P|) d^3\mathbf{r}_P \\ &\sim \int A(\mathbf{r}_P) \delta(\mathbf{r} - \mathbf{r}_P) d^3\mathbf{r}_P \sim A(\mathbf{r}), \end{aligned} \quad (2)$$

which is proportional to the field at the object and is non-zero only at the object points. In practice, if one uses a finite number N of wavelengths at regular intervals of $\Delta(1/\lambda)$, then other than the diffraction or defocusing effect of propagation, the object image $A(\mathbf{r})$ repeats itself at a beat wavelength $A = [\Delta(1/\lambda)]^{-1}$, with axial resolution $\delta = A/N$. By use of appropriate values of $\Delta(1/\lambda)$ and N , the beat wavelength A can be matched to the axial extent of the object, and δ to the desired level of axial resolution.

2.2. Variable tomographic scanning in 3D space

In this section, we discuss how to fulfill variable tomographic scanning with scanning directions randomly oriented in 3D space. Rayleigh–Sommerfeld diffraction formula [10] has been used for numerical reconstruction from tilted holograms, but on fixed reconstruction planes [11,12]. We will use it to reconstruct wave distributions in variable tilted planes. Suppose we have extracted the object wave distribution $o(x, y)$ from a hologram, the wave distribution in a variably selected tilted plane can be calculated by the Rayleigh–Sommerfeld diffraction integral as

$$\begin{aligned} E(x_o, y_o, z_o) &= \frac{iE_0}{\lambda} \iint o(x, y) \frac{\exp[ikr(x, y, x_o, y_o)]}{r(x, y, x_o, y_o)} \\ &\quad \times \chi(x, y, x_o, y_o) dx dy, \end{aligned} \quad (3)$$

where k is the wave number given by $k = 2\pi/\lambda$, E_0 is a constant and $\chi(x, y, x_o, y_o)$ is the inclination factor, which is approximately unitary under the Fresnel approximation and is omitted from the following equations. The inverse length $1/r$ can be replaced by $1/r_o$.

As shown in Fig. 1, the hologram (x – y plane) is vertically placed in the $z = 0$ plane. The reconstruction plane x_o – y_o is tilted with its normal direction randomly oriented in space and its origin located at $z = z_o$. The frame x_o – y_o – z_o is defined as Frame {A} in the figure. Now we introduce a new plane x' – y' , parallel to the hologram plane but share the same origin as the x_o – y_o plane, which defines Frame {B}. Any point $[x_o, y_o, z_o]$ on the x_o – y_o plane can be transferred to the new Frame {B} as

$$[x', y', z']^T = {}^B_A R \cdot [x_o, y_o, z_o]^T, \quad (4)$$

where the superscript T represents the vector transpose. z_o is set to be zero for all the points on the x_o – y_o plane since the plane is vertical to the z_o axis and it passes through the origin of {A}. ${}^B_A R$ is the transform matrix of Frame {A} relative to Frame {B}, and can be expressed as

$${}^B_A R = \begin{bmatrix} t_{11} & t_{12} & t_{13} \\ t_{21} & t_{22} & t_{23} \\ t_{31} & t_{32} & t_{33} \end{bmatrix}. \quad (5)$$

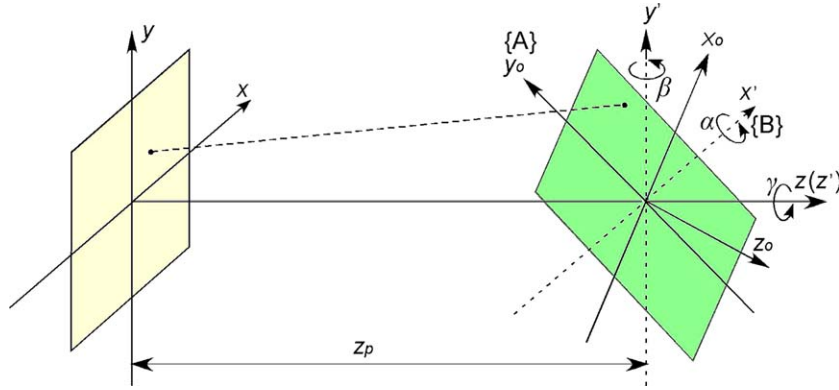


Fig. 1. Reconstruction of the wavefield on a tilted x_o - y_o plane for a given wave distribution on the x - y plane (hologram plane).

For example, if Frame {A} is obtained by rotating Frame {B} about x' -axis by an angle α , then rotating about y' by an angle β , and then rotating about z by an angle γ , the total transform matrix ${}^B_A R$ can be expressed as

$${}^B_A R = R_{z'}(\gamma)R_{y'}(\beta)R_{x'}(\alpha)$$

$$= \begin{bmatrix} \cos \gamma & -\sin \gamma & 0 \\ \sin \gamma & \cos \gamma & 0 \\ 0 & 0 & 1 \end{bmatrix} \begin{bmatrix} \cos \beta & 0 & \sin \beta \\ 0 & 1 & 0 \\ -\sin \beta & 0 & \cos \beta \end{bmatrix}$$

$$\times \begin{bmatrix} 1 & 0 & 0 \\ 0 & \cos \alpha & -\sin \alpha \\ 0 & \sin \alpha & \cos \alpha \end{bmatrix}, \quad (6)$$

where $R_{x_i}(\theta)$ represents the transfer matrix of a rotation about an axis x_i by an amount of θ . The positive directions of the rotation angles around different axes are also shown in Fig. 1. the distance $r(x, y, z, x_o, y_o, z_o)$ between any point (x, y, z) on the hologram plane and a point (x_o, y_o, z_o) on the destination reconstruction plane can be calculated as

$$r = \sqrt{(z_p + z')^2 + (x - x')^2 + (y - y')^2}$$

$$= \sqrt{x^2 + y^2 + z_p^2 + x'^2 + y'^2 + z'^2 - 2xx' - 2yy' + 2z_p z'}$$

$$= \sqrt{x^2 + y^2 + z_p^2 + x_o^2 + y_o^2 - 2xx' - 2yy' + 2z_p z'}, \quad (7)$$

where we have substituted $x'^2 + y'^2 + z'^2$ with $x_o^2 + y_o^2$, which is obvious from Eq. (4) according to the property of rotation matrix. The above square root can be expanded as a power series of $r_o = (z_p^2 + x_o^2 + y_o^2)^{1/2}$. If only the first two lower order terms in the expanded series are considered, then Eq. (7) can be expressed as

$$r \approx r_o \left(1 + \frac{(x^2 + y^2 - 2xx' - 2yy' + 2z_p z')}{2r_o^2} \right), \quad (8)$$

which is substituted into the Rayleigh–Sommerfeld diffraction integral of Eq. (3). We also substitute x' , y' and z' with x and y from Eqs. (4) and (5), and finally we get

$$E(\xi, \eta, z_o) = \frac{iE_0}{\lambda r_o} \exp \left[ikr_o + \frac{ik}{r_o} (t_{31}x_o + t_{32}y_o)z_p \right]$$

$$\times \iint o(x, y) \exp \left[\frac{ik}{2z_o} (x^2 + y^2) \right]$$

$$\times \exp[-i2\pi(\xi x + \eta y)] dx dy, \quad (9)$$

with

$$\xi = \frac{(t_{11}x_o + t_{12}y_o)}{\lambda r_o}, \quad (10)$$

$$\eta = \frac{(t_{21}x_o + t_{22}y_o)}{\lambda r_o}. \quad (11)$$

Here we have introduced a further approximation, $ik(x^2 + y^2)/2r_o \approx ik(x^2 + y^2)/2z_o$, which holds almost the same restriction as the Fresnel condition. This approximation is introduced to simplify the calculation of Eq. (9), so that it can be implemented with the fast Fourier transform (FFT) algorithm. And finally a coordinate transform is made to get the wave distribution in the (x_o, y_o) coordinate as indicated in Eqs. (10) and (11). In the discrete implementation of Eq. (9), we have the following relationship according to the Shannon theory:

$$t_{11}\Delta x_o + t_{12}\Delta y_o = \frac{\lambda r_o}{N\Delta x}, \quad \text{and} \quad t_{21}\Delta x_o + t_{22}\Delta y_o = \frac{\lambda r_o}{N\Delta y}, \quad (12)$$

where Δx_o and Δy_o are the resolutions of the tilted plane, Δx and Δy are the resolutions of the hologram plane and $N \times N$ is the array size of a square area on the CCD, thus the resolution of the reconstructed plane can be analytically calculated from the given Δx and Δy .

It is interesting to note that if the rotation angles β and γ are both set to be zero in Eq. (6), Eq. (9) can be written as

$$E(\xi, \eta, z_o) = \frac{iE_0}{\lambda r_o} \exp \left[ik \left(r_o + \frac{z_p y_o \sin \alpha}{r_o} \right) \right]$$

$$\times \iint o(x, y) \exp \left[\frac{ik}{2r_o} (x^2 + y^2) \right]$$

$$\times \exp \left[-i2\pi \left(\frac{x_o}{\lambda r_o} x + \frac{y_o \cos \alpha}{\lambda r_o} y \right) \right] dx dy, \quad (13)$$

with the resolution of the reconstruction plane as

$$\Delta x_o = \frac{\lambda z}{N \Delta x} \quad \text{and} \quad \Delta y_o = \frac{\lambda z}{N \Delta y \cos \theta}, \quad (14)$$

which is obvious from Eq. (12). In this case, the normal direction of the reconstruction plane is located in the y - z plane. This is exactly the case discussed in Ref. [9]. And furthermore, if all the rotation angles α , β , and γ are set to be zero, Eq. (9) can be further simplified as the well-known Fresnel diffraction formula [13], where all the reconstruction planes are perpendicular to the optical axis.

3. Experiments and discussion

In this section, experiments are performed to verify the proposed algorithm for variable tomographic scanning. The optical setup of the experiment is based on a Michelson interferometer, as shown in Fig. 2. A coherent 699 ring dye laser, with a continuously tunable wavelength from 567.0 to 613.0 nm, is used for illumination. The laser beam is split at beam splitter BS into reference and object beams, and each part is focused by lens $L1$ onto the focal point $F1$ or $F2$. Point $F2$ is also the front focus of objective $L2$, so the object is illuminated with a collimated beam. The plane S is imaged to the CCD camera by the lens $L2$. In the reference arm the beam is also collimated by lens $L3$, which results in a magnified image at the CCD camera of an interference pattern that would exist at S if the object wave is superposed with a plane wave there. An aperture AP is placed in the focal plane of $L2$ to control the size of the object angular spectrum captured in the CCD camera. An off-axis hologram arrangement is used by slightly tilting the reference mirror REF. As we know for off-axis holography, the object angular spectrum can be separated from other spectral components of the hologram with a band-pass filter if the off-axis angle of the two beams is properly adjusted. Then, the pure object wave distribution $o(x,y)$ on the hologram plane can be readily extracted by taking an inverse Fourier transform of the object spectrum [13].

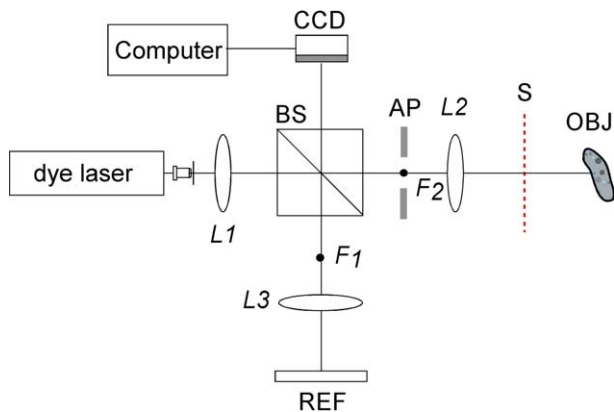


Fig. 2. Optical apparatus used in the digital interference holography experiments.

The WSDIH system is used to image a tilted 25 cent coin, rotated from x' - y' plane with $\alpha = -4^\circ$, $\beta = 7.5^\circ$ and $\gamma = 0^\circ$ in space, as shown in Fig. 1. The selected area on the coin surface contains two letters “OR”, and has a size of $2.5 \times 2.5 \text{ mm}^2$ with 300×300 pixels. The coin can be viewed as an object with two surfaces: the base surface of the coin and the top surface of the letters. The reconstruction distance z , representing the distance from the object to S plane in Fig. 2 is set to be 36 mm. The wavelengths of the dye laser is scanned for a range of 580.0–590.0 nm at 20 values, which gives an axial range of 650 μm and axial resolution of 32 μm according to Section 2.1.

For comparison, the Fresnel diffraction formula is first used to reconstruct the wave fields for scanning direction normal to the hologram plane. Thus the reconstruction x_o - y_o planes are all parallel to the hologram plane. The wave distributions from all the holograms are numerically superposed together to obtain the accumulated field distribution that represents the three-dimensional object structure. Fig. 3(a) shows four contour images at different layers of the object at about 60 μm axial distance intervals. Since the coin is tilted relative to the hologram plane in both directions, the contours are all tilted in the images, and they sequentially appear from left top to right bottom in Fig. 3(a) as the distance z is increased. Fig. 4(a) is the flat view of all the y_o - z_o cross-sections from the reconstructed volume and Fig. 4(b) is the x_o - z_o flat view. Since the coin is tilted in both directions relative to x_o - and y_o -axes, so it is not parallel to the scanning planes, and one can clearly see the extended width (or thickness) of the flat views in both figures. We have used the proposed algorithm of Eqs. (9)–(11) for reconstruction but with $\alpha = 0$, $\beta = 0^\circ$ and $\gamma = 0^\circ$, and obtained the same results as above, proving the fact that the Fresnel diffraction formula is only a special case of the proposed algorithm.

Using the known orientation of the coin in space, we can set proper angles for scanning in the algorithm. If we choose $\alpha = 0$ and $\beta = 7.5^\circ$, then the reconstruction plane is tilted in space, and has a relative 4° angle to the coin surface around the x_o -axis. Fig. 3(b) shows another four contour images, which now sequentially appear from top to bottom as the distance z is increased. The y_o - z_o flat view in Fig. 4(c) now shrinks to two relative thin lines, which represent the two surfaces of the coin. This reflects the fact that the reconstruction angle of $\beta = 7.5^\circ$ matches the orientation of the coin in space. However, the x_o - z_o flat view in Fig. 4(d) of the cross-sections is almost as thick as Fig. 4(b), since we have selected the reconstruction angle $\alpha = 0$ so that the reconstruction plane still has a relative angle to the coin surface around x_o -axis.

Now we choose the scanning plane parallel to the base surface of the coin, so that the features of the relief appear simultaneously in a single tomographic scanning. Specifically, the rotation angles of the reconstruction plane are set to be $\alpha = -4^\circ$ and $\beta = 7.5^\circ$, as shown in Fig. 1. The reconstructed contour images are shown in Fig. 3(c), from which we can see that the letters on the coin are now either

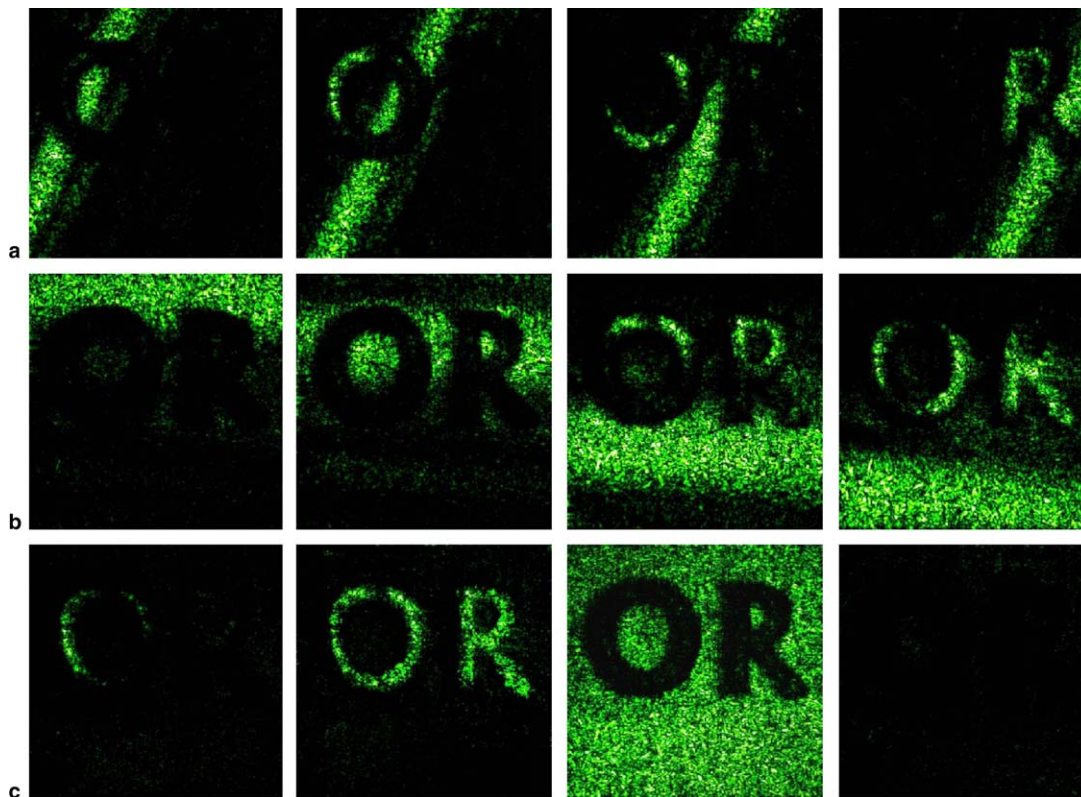


Fig. 3. Reconstruction of contour images of a quarter in a $2.5 \times 2.5 \times 0.65 \text{ mm}^3$ volume with tilted angles: (a) $\alpha = 0^\circ$, $\beta = 0^\circ$, $\gamma = 0^\circ$; (b) $\alpha = 0^\circ$, $\beta = 7.5^\circ$, $\gamma = 0^\circ$ and (c) $\alpha = -4^\circ$, $\beta = 7.5^\circ$, $\gamma = 0^\circ$.

all highlighted or all darkened, for they are located in the same scanning plane. Similarly, Fig. 4(e) shows the y_o-z_o flat view of the reconstruction and Fig. 4(f) is the x_o-z_o flat view. Clearly, both of the above two flat views shrink to two thin lines since the scanning plane are now parallel to the coin base surface and the reconstruction angles match well with the actual orientation of the coin.

In the above we have used rotation angles α and β to adjust the orientation of the scanning plane. Angle γ can also be used to rotate the reconstructed features. Fig. 5(a) shows several contour images at about $60 \mu\text{m}$ axial distance intervals with $\alpha = 0^\circ$, $\beta = 7.5^\circ$ and $\gamma = 30^\circ$; and Fig. 5(b) shows the reconstruction results with $\alpha = -4^\circ$, $\beta = 7.5^\circ$ and $\gamma = 160^\circ$.

The above experiments clearly demonstrate the effectiveness of the proposed algorithm. The rotation angle γ in the algorithm can be any angle within 360° . The Fresnel approximate conditions will impose a restriction to the extent of the tilted reconstruction plane, which is related to the tilted angles α or β . In the case of Eq. (13), the reconstruction plane is tilted only around x' axis. And according to numerical analysis, we find that tilted angle α can be selected as large as 60° and good reconstruction can still be achieved.

As in most of the 3D microscopy systems, the 3D volume can be reconstructed as a set of scanning planes perpendicular to the optical axis. If the lateral resolution is comparable to the axial resolution, a tilted tomographic image can

be obtained by combining or interpolating points from different tomographic layers without too much sacrifice of the image quality. However, if the lateral resolution does not match well with the axial resolution, the quality of the interpolated image will be greatly degraded. For example, if the lateral resolution is much better than the axial resolution, each point on a tiled plane need to be interpolated from points of two nearby tomographic layers, and these points are separated with a relatively large axial distance compared to its original lateral resolution, thus the interpolated point on the tiled plane will lose its accuracy because of the poor axial resolution of the system. As in WSDIH system, the axial resolution is determined by the wavelength scanning range of the dye laser system and is typically $\sim 10 \mu\text{m}$ [7,8]. However, the lateral resolution can be much higher (for example, $\sim 1 \mu\text{m}$) if microscopic objectives with high magnification are used in the optical system. Thus a direct interpolation will cause significant degradation to the images in this case.

The intention of using WSDIH for variable tomographic scanning in this paper is based on the advantage of digital holography, that the holograms have recorded all the information of the object. Thus it is possible to directly calculate the more rigorous wavefield distributions on a tilted plane from the recorded holograms. And the numerical superposition of these more rigorous tilted fields results in tilted tomographic images, which will thus have

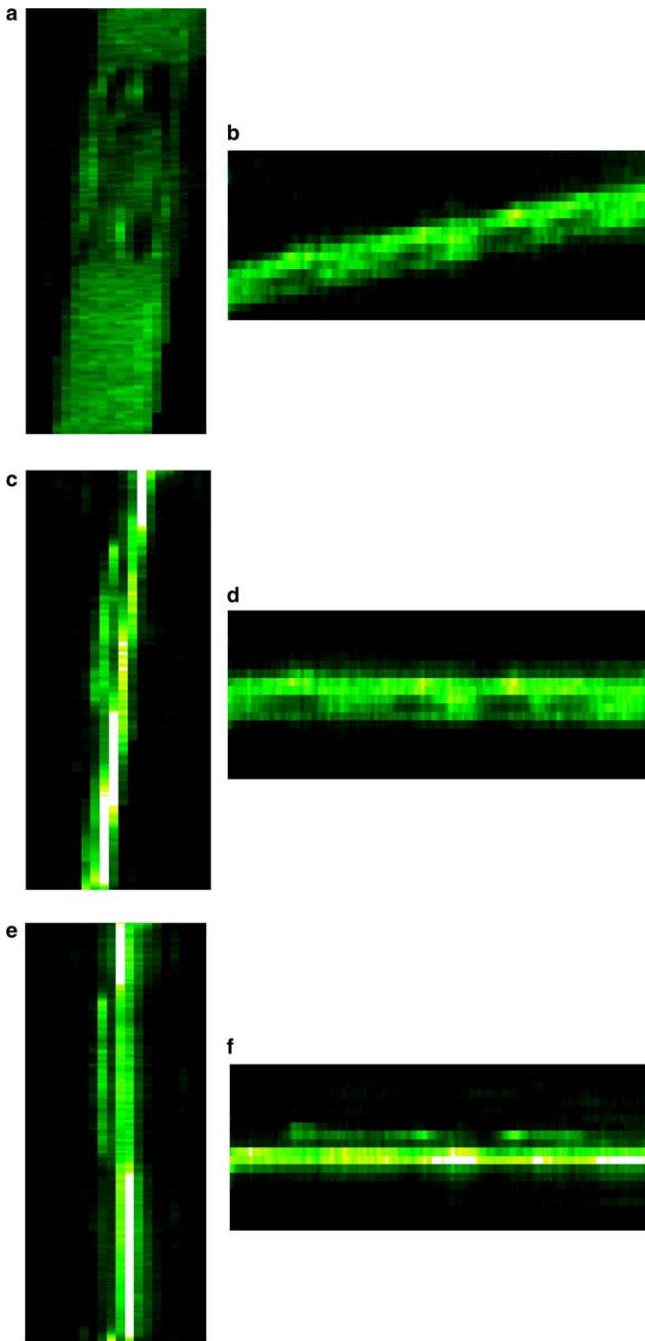


Fig. 4. (a), (c) and (e) are flats views of the y_o - z_o cross-sections from Figs. 3(a)–(c), respectively; (b), (d) and (f) are x_o - z_o flats views from Figs. 3(a)–(c), respectively.

better quality than those only from interpolation, especially when the lateral resolution does not match well with the axial resolution. Thus the whole process can be fulfilled without physically tilting the object and recording the holograms again, which is a unique capability not available in other tomographic imaging systems.

The current method introduces some approximate conditions as well, and these approximations are mainly introduced for the fast implementation of the algorithm. In order to reconstruct the wavefield on tilted planes, it

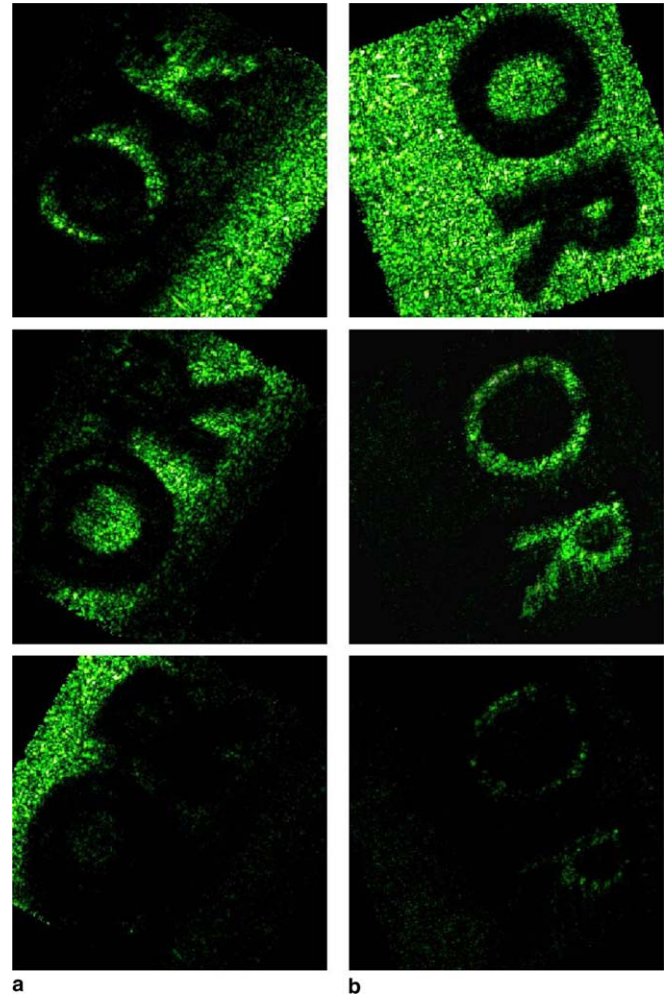


Fig. 5. Contour images at about $60\ \mu\text{m}$ axial distance intervals with (a) $\alpha = 0^\circ$, $\beta = 7.5^\circ$, $\gamma = 30^\circ$ and (b) $\alpha = -4^\circ$, $\beta = 7.5^\circ$, $\gamma = 160^\circ$.

is normally inevitable to introduce a coordinate transform, either in the space domain [9,11,12] or in the spectrum domain [14]. However, it is possible to introduce less or no other approximations to the algorithm. The authors are currently developing more rigorous algorithms for tilted reconstructions, which will be reported in the near future. For more discussions about the acquisition speed and the sensitivity of the WSDIH system, readers can refer to Ref. [9].

4. Conclusion

In conclusion, we have proposed an algorithm for variable tomographic scanning based on the principle of wavelength scanning digital holography. Object fields are reconstructed in a number of selected tilted planes from a series of holograms and the numerical superposition of the tilted image volumes result in the variable tomographic scanning. In the proposed algorithm, the reconstruction angles can be selected as arbitrarily angles in space and not limited in a two-dimensional plane. It will offer more flexibility to observe randomly oriented structures and

features of a specimen in a WSDIH system. Experimental results are presented to demonstrate the effectiveness of the method.

Acknowledgements

This work is supported in part by the National Science Foundation. L. Yu gratefully acknowledges the financial support of the German Alexander von Humboldt Foundation.

References

- [1] D. Huang, E.A. Swanson, C.P. Lin, J.S. Schuman, W.G. Stinson, W. Chang, M.R. Hee, T. Flotte, K. Gregory, C.A. Puliafito, J.G. Fujimoto, *Science* 254 (1991) 1178.
- [2] A. Dubois, K. Grieve, G. Moneron, R. Lecaque, L. Vabre, C. Boccara, *Appl. Opt.* 43 (2004) 2874.
- [3] E. Bordenave, E. Abraham, G. Jonusauskas, N. Tsurumachi, J. Oberle, C. Rulliere, P.E. Minot, M. Lassegues, J.E.S. Bazeille, *Appl. Opt.* 41 (2002) 2059.
- [4] B. Laude, A. De Martino, B. Drevillon, L. Benattar, L. Schwartz, *Appl. Opt.* 41 (2002) 6637.
- [5] M. Ducros, M. Laubscher, B. Karamata, S. Bourquin, T. Lasser, R.P. Salathe, *Opt. Commun.* 202 (2002) 29.
- [6] L. Yu, M.K. Kim, *Opt. Exp.* 12 (2004) 6632.
- [7] M.K. Kim, *Opt. Exp.* 7 (2000) 305.
- [8] M.K. Kim, *Opt. Lett.* 24 (1999) 1693.
- [9] L. Yu, M.K. Kim, *Opt. Exp.* 13 (2005) 5621.
- [10] J.W. Goodman, *Introduction to Fourier Optics*, McGraw-Hill, 1996.
- [11] D. Leseberg, C. Frere, *Appl. Opt.* 27 (1988) 3020.
- [12] L. Yu, Y. An, L. Cai, *Opt. Exp.* 10 (2002) 1250.
- [13] U. Schnars, W. Juptner, *Meas. Sci. Technol.* 13 (2002) 85.
- [14] K. Matsushima, H. Schimmel, F. Wyrowski, *JOSA A* 20 (2003) 1755.